ORIGINAL ARTICLE

Tracking climate change in the spatial distribution pattern and the phylogeographic structure of Hyrcanian wood frog, *Rana pseudodalmatina* (Anura: Ranidae)

Negar Amiri[1] | Somaye Vaissi[2] | Fateme Aghamir[3] | Reihaneh Saberi-Pirooz[1] | Dennis Rödder[4] | Elham Ebrahimi[1] | Faraham Ahmadzadeh[1]

[1]Department of Biodiversity and Ecosystem Management, Environmental Sciences Research Institute, Shahid Beheshti University, Tehran, Iran

[2]Department of Biology, Faculty of Science, Razi University, Kermanshah, Iran

[3]Department of Agroecology, Environmental Sciences Research Institute, Shahid Beheshti University, Tehran, Iran

[4]Herpetology Section, Zoologisches Forschungsmuseum Alexander Koenig (ZFMK), Bonn, Germany

Correspondence
Faraham Ahmadzadeh, Department of Biodiversity and Ecosystem Management, Environmental Sciences Research Institute, Shahid Beheshti University, G.C., Evin, Tehran, Iran.
Email: f_ahmadzade@sbu.ac.ir

Abstract

Climate change has essential effects on patterns of population persistence, connectivity, and divergence. We used mtDNA sequences and species distribution modeling to assess the impact of climatic changes in the past (Last Glacial Maximum [LGM: 21 Kya] and Mid-Holocene [6 Kya]), recent (1970–2000), and future (2070) on the phylogeography and spatial distribution of populations of the Hyrcanian wood frog, *Rana pseudodalmatina*, in northern Iran. Based on two mitochondrial genes (*cytochrome b* and *16S* ribosomal RNA), we found evidence for two regional patterns that diverged in the Pleistocene (1.6 Mya) and are distributed in the eastern and western sections of the current species range. Biogeographic analyses support the hypothesis that both vicariance (an increase in the Caspian Sea water levels) and dispersal events have been involved in shaping the species' genetic structure. Reconstruction of the ancestral distribution of *R. pseudodalmatina* suggests the species' range contracted in two independent eastern and western glacial refugia during the LGM, expanding from the Mid-Holocene to the present to occupy Hyrcanian forests continuously. According to future climate projections, the species' range shows a tendency to shift to higher altitudes. Landscape connectivity analyses support higher population continuity in the central part of the current range, with isolated populations in the easternmost and westernmost extremes. Our integrative study of *R. pseudodalmatina* provides support for the "refugia-within-refugia" scenario in the Hyrcanian forests.

KEYWORDS
conservation, future distribution, landscape connectivity, quaternary climate change, refugia-within-refugia

1 | INTRODUCTION

Climatic changes through time have important effects on the evolutionary history and spatial distribution of species (Bontrager & Angert, 2019; Foden et al., 2013; Hopley & Byrne, 2019; Omann et al., 2009; Razgour et al., 2019; Velásquez-Tibata et al., 2012; Vieira et al., 2018). Historical changes in regional climate also play an important role in conditioning patterns of gene flow among

populations, with species-specific life histories and demographics also contributing to shaping species distributions and their temporal dynamics (Baek et al., 2018; Bell et al., 2010; Hua, 2013; Safner et al., 2011; Schierenbeck, 2017). Numerous phylogeographic studies have shown that during cold phases of the last glacial period the distribution ranges of many species contracted to climatic refugia (Bao et al., 2015; Leipold et al., 2017; Malekoutian et al., 2020; Song et al., 2018). Subsequently, as temperatures increased during the Holocene, distributions expanded again to occupy newly suitable habitats (Chen et al., 2017; Cox et al., 2019; Igea et al., 2013; Liepelt et al., 2009; Zhao et al., 2019). On shorter, more recent time scales, climate change has been linked to distribution shifts in many species, sometimes resulting in local or regional extinction (Devictor et al., 2012; He et al., 2018; McCarty, 2001). According to 131 studies, extinction rates in response to climate change are estimated to range from 0% to 54%, with an average of 7.9% (Urban, 2015). Therefore, understanding how species respond to climate change is of fundamental importance in conservation planning.

Identifying Quaternary climatic refugia due to stable climatic conditions can be critical to the conservation of species for future climate change in terms of predicting the effects on population persistence (Provan & Bennett, 2008), especially in globally threatened groups like amphibians (Alroy, 2015; Duarte et al., 2012; Pounds et al., 2006). Due to their biphasic life-cycles, highly permeable skin, and unshelled eggs, amphibians are particularly vulnerable to alterations in environmental conditions, and climate change has been identified as one of the most important factors threatening their populations (Carey & Alexander, 2003; Corn, 2005; Wake & Vredenburg, 2008). Amphibians are regarded as good bioindicators of environmental changes due to their physiological constraints and relatively low mobility (Carnaval et al., 2009). Genetic studies can provide evidence for historical distribution shifts of amphibian populations in response to climatic oscillations during the Quaternary (Afroosheh et al., 2019; Chiocchio et al., 2017; Fouquet et al., 2012; Provan & Bennett, 2008; Yodthong et al., 2015; Zeisset & Beebee, 2008; Zhang et al., 2016; Zhou et al., 2014). Integrative studies combining phylogeographic analyses with species distribution modeling (SDM) can be used to assess the impact of past climatic changes on the evolutionary history and historical demography of populations and help predict future changes in their geographical ranges (Afroosheh et al., 2019; Ahmadzadeh et al., 2013; Nicolas et al., 2018; Velo-Antón et al., 2013).

The Hyrcanian wood frog, *Rana pseudodalmatina* Eiselt & Schmidtler, 1971, is a brown frog (Anura, Ranidae) endemic to temperate forests in northern Iran (also known as Hyrcanian forests). It ranges from the Talesh region to the Golestan National Park, on the northern slopes of the Alborz Mountains and the southern edge of the Caspian Sea of Iran (Najibzadeh et al., 2018). The species composition and diversity of the Southwest Asian forests, rich in endemic species, suggests that the Hyrcanian region has likely acted as a glacial refugium for many taxa during the Quaternary glaciations (Röhrig, 1991; Saberi-Pirooz et al., 2018). Phylogeographic studies and climatic models have shown that the southern Caspian Sea has acted as a glacial refugium

for a broad range of taxa, including Iranian rock lizards (*Darevskia chlorogaster* and *Darevskia defilippii*, Ahmadzadeh, Flecks, et al., 2013), Iranian brown bears (*Ursus arctos*, Ashrafzadeh et al., 2016), fat dormouse (*Glis glis*, Ahmadi et al., 2018), Persian mountain salamanders (*Paradactylodon persicus*, Ahmadzadeh et al., 2020), and Caspian green lizard (*Lacerta strigata*, Saberi-Pirooz et al., 2021). During the last half-century, the climate became warmer in the Hyrcanian forests, with the average annual temperature increasing between 1.28 and 2.45℃ and annual precipitation declining between 55.6 and 409.4 mm (Tohidifar et al., 2016). Due to the close relationship between temperature and rainfall and amphibian distributions (Ortiz-Yusty et al., 2013), this warming trend is expected to have a negative impact on the distribution of *R. pseudodalmatina*. This species is categorized as Least Concern (LC) in the IUCN Red List, but few studies have assessed the species' conservation status and threats (Sharifi et al., 2009).

The main aims of this study are (a) to investigate the evolutionary history and demographic history of *R. pseudodalmatina* based on two mitochondrial DNA fragments (*cytochrome b*, *cytb*, and *16S* ribosomal RNA, *16S*); (b) to assess the impact of past (Last Glacial Maximum and Mid-Holocene) and more recent (1970–2000) climate fluctuations on the spatial distribution pattern of the species using Species Distribution Models (SDMs); and (c) to investigate whether *R. pseudodalmatina* will behave as a single distributional unit in response to future climate change (2070).

2 | MATERIALS AND METHODS

2.1 | Sampling

Twenty specimens of *R. pseudodalmatina* and five specimens of *Rana macrocnemis* were collected across their distribution range in the Hyrcanian forests (Figure 1, Appendix 1). Tissue samples consisted of third toe clips; all sampled individuals were subsequently released at the site of capture. Samples were preserved in 96% ethanol and kept at −20℃ prior to DNA extraction. Details of sampling locations, accession numbers for newly generated mtDNA sequences, and code ID are presented in Appendix 1.

2.2 | Laboratory procedures and sequence analysis

DNA was extracted following a standard high-salt protocol (Sambrook, 1989). The primers L14841 (Kocher et al., 1989)/CB3H and 16SA/16SB (Palumbi et al., 1991) were used to amplify fragments of two mitochondrial genes: *Cytochrome b* (*cytb*; 700 bp) and *16S* ribosomal RNA (*16S*; 560 bp), respectively (Table S1). PCRs were run in a total volume of 25 μl containing 12.5 μl of Master Mix Red (Ampliqon), 0.5 μl of each primer (10 μM), 10.5 μl ddH$_2$O, and 1 μl of template DNA. Amplification of each gene was carried out under the conditions described in Veith et al. (2003) (see Table S1). PCR amplifications were visualized on 1% agarose gels including negative controls. PCR products were sequenced by Macrogen Inc. Chromatographs were checked and

edited using Codon-Code Aligner v.6.0.2.X (CodonCode Corporation). All new sequences were submitted to GenBank (Appendix 1).

2.3 | Phylogenetic analysis

For phylogenetic analysis, some sequences were obtained from the NCBI (www.ncbi.nlm.nih.gov) and were added to our dataset (see Appendix 1). The sequences of the two mtDNA genes (*cytb* and *16S*) were aligned with MAFFT v.6 (Katoh et al., 2017) (https://mafft.cbrc.jp/; algorithm: Auto; scoring matrix: 200 Pam/$k = 2$; Gap open penalty: 1.53) and were then combined, resulting in a 937 bp alignment (*cytb*: 442 bp; Alignment S1 and *16S*: 495 bp; Alignment S2). The best-fit model was selected using MrModeltest v.2.3 (Nylander, 2004) under Akaike's information criterion (Akaike, 1974). GTR+G+I (Rodriguez et al., 1990; Yang, 1996) was selected as the best-fit model for both *cytb* and *16S* genes ($G = 1.05$ and *p*-inv = 0.55; $G = 0.47$ and *p*-inv = 0.41). A maximum likelihood (ML) tree was reconstructed using RAxML v.7.2 (Stamatakis, 2006) under the GTR+G+I model with 1000 bootstrap pseudoreplicates to assess branch support. The Bayesian inference (BI) analysis was performed using MrBayes v.3.2 (Huelsenbeck & Ronquist, 2001) with two simultaneous runs and four chains with 10^7 generations. We subsampled trees and parameters every 100th generation, which produced 10^5 trees. The first 10% of these trees were discarded as burn-in, and the remaining trees were used to reconstruct a consensus tree. The final standard deviation (SD) of split frequencies for the combined dataset (two genes) was 0.0015. The parameters were separately calculated for each gene partition. We assessed run performance, convergence of parameters, and effective sample size (ESS) with Tracer v.1.6 (Rambaut et al., 2007). The statistical significance of alternative tree topologies using the Shimodaira-Hasegawa (SH) (Shimodaira & Hasegawa, 1999) was evaluated with 1000 bootstrap pseudoreplicates likelihood ratio test (SH-aLRT; Anisimova et al., 2011) as implemented in IQ-Tree v.1.6.12 (Nguyen et al., 2015).

Uncorrected *p*-distances between two western and eastern groups (see results) were calculated with PAUP v.4.0a10 (Swofford, 2002) for each mtDNA gene separately.

2.4 | Estimating divergence time

The divergence times were estimated with BEAST v.1.7.2 (Drummond & Rambaut, 2007) using the combined data set (*cytb* and *16S*). For calibration of the molecular clock, a secondary calibration approach was taken based on two calibration points: first, we set the age for the *R. pseudodalmatina*/*R. macrocnemis* – *Rana tavasensis* clade at 5.18 million years ago (Mya) based on Ehl et al. (2019); and second, we set the time of the most recent common ancestor (henceforth MRCA) of *Rana arvalis*, *Rana temporaria*, and *Rana pyrenaica* at 7.68 Mya, based on Ehl et al. (2019). These calibration points were applied as follows: first node, normal distribution, mean:

5.18 Mya, standard deviation: 1.42 Mya; second node, normal distribution, mean: 7.68 Mya, standard deviation: 1.68 Mya. Analyses were run under a lognormal relaxed clock (uncorrelated) model, because primary runs using an uncorrelated lognormal clock revealed ucld. stdev ($\delta > 0.1$) for all genes. The Yule process was used as a prior for the speciation process. The analysis was run for 3×10^7 generations, sampling trees and parameters every 10^3 generations. Tracer v.1.5 was used to assess convergence and effective sample sizes (ESS) of parameter estimates.

2.5 | Genetic structure and demographic analysis

An analysis of molecular variance (AMOVA) was conducted based on standardized estimates of genetic differentiation (F_{st}) with 10,000 permutations to assess genetic structure in *R. pseudodalmatina* using Arlequin v.3.5 (Excoffier & Lischer, 2010). Molecular diversity indices, including the number of haplotypes (H), haplotype diversity (*h*), and nucleotide diversity (π), were assessed for both markers separately using the same program.

The historical demography of the two regional patterns (see results) in *R. pseudodalmatina* was investigated with neutrality analyses, calculating Tajima's *D* and Fu's *Fs* indices with Arlequin v.3.5. Additionally, mismatch distributions (MMD) were reconstructed using the same software, comparing the frequency distribution of pairwise nucleotide differences in *cytb* sequences in each regional pattern, with that expected under sudden demographic expansion.

As a complementary approach, we reconstructed the Bayesian skyline plots (BSP; Drummond et al., 2005) to investigate the variations in effective population size (henceforth N_e) through time, in each regional pattern, using *cytb* sequences. The analysis was conducted with BEAST v1.7.2 under a strict molecular clock model with a fixed rate of 1.8×10^{-2} substitutions per site per Mya (estimated for the related brown frog *R. arvalis*, Babik et al., 2004). The analysis was run for 5×10^6 generations with parameters sampled every 100 iterations. The parsimony haplotype network was constructed using TCS v.1.21 (Clement et al., 2000) for the *cytb* sequences under the 95% limit of parsimony.

2.6 | Biogeographic analysis

Based on the results of phylogenetic analyses (see section 3), the distribution of *R. pseudodalmatina* can be divided into two areas, corresponding to the western (W) and eastern (E) sections of the species range. The statistical dispersal-vicariance analysis (S-DIVA) and Bayesian binary MCMC (BBM) analysis were used to reconstruct the possible ancestral range for *R. pseudodalmatina*. The analysis was implemented using RASP v.2.1 beta (Yu et al., 2015) using *cytb* sequences. Because this analysis requires a fully resolved topology, we used a reduced tree including only haplotypes (see Appendix 1) as input for the analysis. The haplotype tree was used as input for the analysis. To consider phylogenetic uncertainty, 20,000 of the

posterior trees sampled during the BI analyses were used as the input file for S-DIVA. The BBM analysis was run for 5×10^6 generations under 10 MCMC, and the sampling frequency was every 100 generations. The fixed Jukes-Cantor model with equal among-site rate variation was used for the BBM analysis.

2.7 | Potential distribution analysis (past–present–future)

2.7.1 | Species record, climate data, and variable selection

We compiled information on georeferenced localities of *R. pseudodalmatina* from our own fieldwork and literature sources (Appendix 1). When no coordinates were provided in literature sources, we georeferenced the observations using the Biogeomancer Software (http://bg.berkeley.edu/latest/). In total, 41 unique records were available for model building covering the whole known geographic range of the species, which were mapped in ArcGIS v.10.8 to spot potential errors.

Climatic information characterizing current climatic conditions was obtained from WorldClim.org v.2.0 in terms of 19 bioclimatic predictors with a spatial resolution of 2.5 arc.min (Fick & Hijmans, 2017). To reduce the multi-collinearity of predictors, we used the SDMtune package for Cran R (Vignali et al., 2020) to identify a set of variables that have low collinearity and at the same time a high predictive ability for the study species. The final set of variables were as follows: BIO7 = Temperature Annual Range; BIO8 = Mean Temperature of Wettest Quarter; BIO9 = Mean Temperature of Driest Quarter; BIO13 = Precipitation of Wettest Month.

To estimate past and future range dynamics, we followed two different approaches: (a) We used downscaled global circulation model outputs for the time slices Mid-Holocene (6 ky BP) and at the Last Glacial Maximum (LGM; 21 ky BP) as unweighted ensembles based on palaeoclimate simulations following the r1i1p1 ensemble from the PMIP3 project (Paleoclimate Modeling Intercomparison Project Phase III, https://pmip3.lsce.ipsl.fr/; (Braconnot et al., 2012). A total of 11 scenarios were available as estimates of Mid-Holocene climate (MRICGCM3, MPI-ESM-P, MIROC-ESM, IPSL-CM5A-LR, GISS-E2-R, FGOALS-g2, CSIRO-Mk3l-1-2, CSIRO-Mk3-0, CNRM-CM5, CCSM4, and BCC-CSM1-1) and seven scenarios were available for the LGM (MRI-CGCM3, MPI-ESM-P, MIROC-ESM, IPSL-CM5A-LR, FGOALS-g2, CNRM-CM5, and CCSM4). To evaluate the potential future distribution in 2070, we used averages of four IPCC 5 storylines RCP 2.6, RCP 4.5, RCP 6, and RCP 8.5 as suggested by 10 GCMs (NorESM1-M, MRI-CGCM3, MIROC5, MIROC-ESM, MIROC-ESM-CHEM, IPSL-CM5A-LR, HadGEM2-ES, HadGEM2-AO, GISS-E2-R, CCSM4, and BCC-CSM1-1). The downscaling procedure to 2.5 arc.min is described in Krehenwinkel et al. (2016). (b) As the second climate data set we used Oscillayers provided by Gamisch (2019). This dataset comprises 256-time slices in steps of 10 ky characterizing climatic oscillations within the Pleistocene. For each time slice, 19 bioclimatic variables with a spatial resolution of 2.5 arc.min are available which are conceptually equivalent to those available from WorldClim.

2.7.2 | Species distribution modeling

For SDM development, we used MaxEnt v.3.4.4 (Phillips et al., 2006, 2017), which is a presence-pseudoabsence method and allows an estimation of potentially suitable habitats (Elith et al., 2011). To identify the most suitable settings, we used the relevant functions of the SDMtune package (Vignali et al., 2020), which suggested a regulation parameter of 0.5 and linear, quadratic, and product features. The
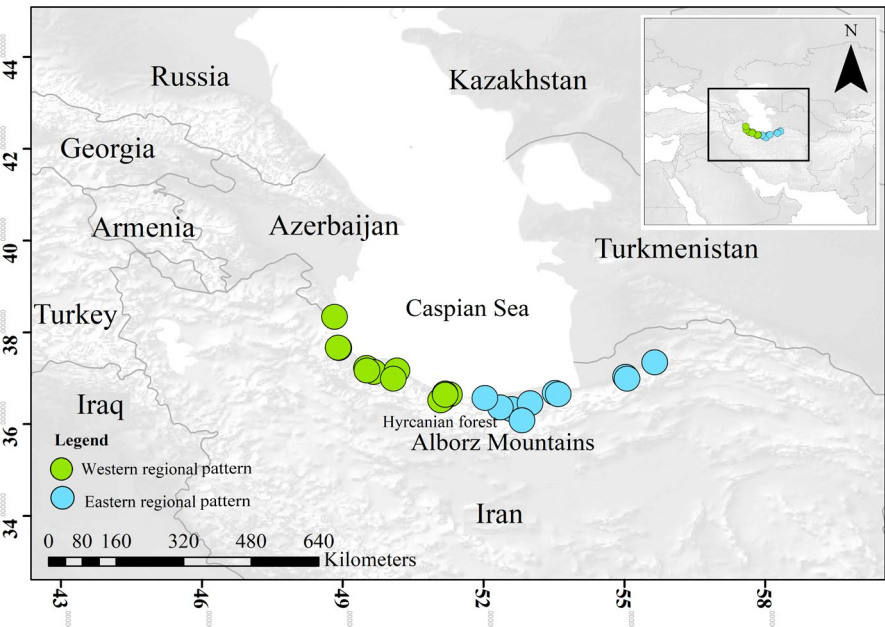

FIGURE 1 Geographical distribution of the Hyrcanian wood frog, *Rana pseudodalmatina* in the Hyrcanian forests. The green circles represent the western regional pattern, and the blue circles represent the eastern regional pattern

TABLE 1 Molecular diversity indices based on *cytb* and *16S* genes within Hyrcanian wood frog, *Rana pseudodalmatina* and western (W) and eastern (E) regional patterns. Sample size (N), number of haplotypes (H), haplotype diversity (*h*), and nucleotide diversity (π)

	Gene	N	H	*h*	π	Tajima's *D*	Fu's *Fs*
Rana pseudodalmatina	cytb	39	12	0.78	0.005	−0.52	−2.07
	16S	48	13	0.69	0.002	−2.15[*]	−9.28[*]
E	cytb	17	4	0.50	0.0008	−1.04	−1.47[*]
	16S	19	6	0.46	0.001	−2.04[*]	−3.86[*]
W	cytb	22	8	0.60	0.001	−2.07[*]	−4.42[*]
	16S	29	7	0.37	0.001	−2.28[*]	−4.68[*]

[*]$p < 0.05$.
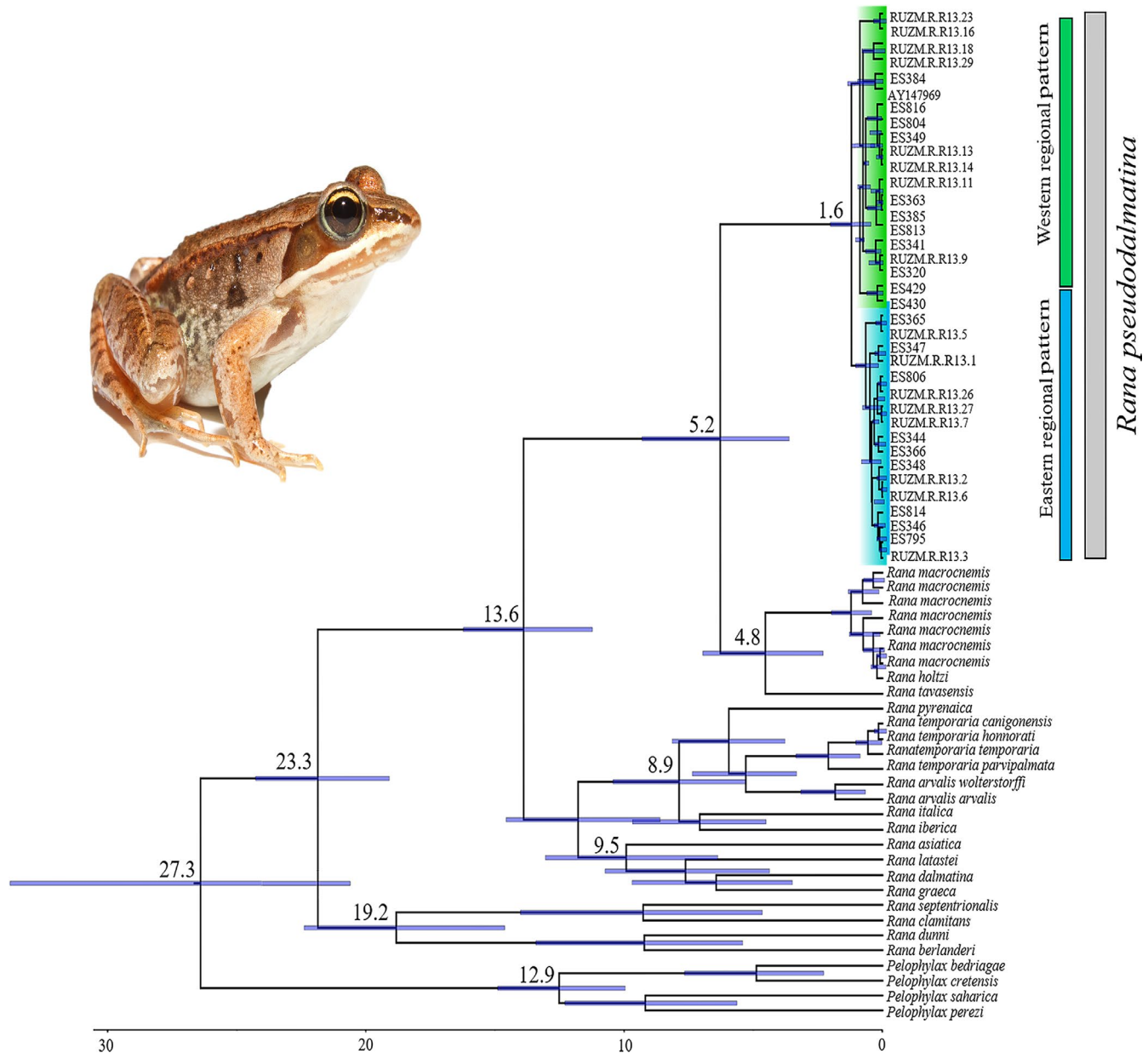
FIGURE 2 A calibration evolutionary time tree based on two mtDNA (*cytb* and *16S*) genes for Ranidae including the genus *Rana*. Blue bars show 95% highest posterior density intervals of the estimated node ages; values indicated on branches are mean node ages (Mya) (photograph by Omid Mozaffari)

total number of species records was 100 times split into 20% used for model testing via the area under the receiver operating characteristic curve (AUC; Swets, 1988) and 80% used for model training applying a bootstrap procedure. Averages across all replicates were projected to current climatic conditions as well as past time slices using the cloglog output format. As environmental background for model training, we selected an area defined by a circular buffer of 75 km enclosing all species records. As a presence–absence threshold, we used an omission threshold of 10% acknowledging potential georeferencing errors. As projecting SDMs through space and time may be subject to extrapolation errors in areas with environmental conditions exceeding the training range of the model, we used multivariate environmental similarity surfaces (MESS; Elith et al., 2010) to quantify areas with increased projection uncertainties. Potential refugia were identified by overlaying all potential distributions as projected onto the oscillayer dataset. Stable refugia were classified as 100% present across all 256-time slices, 99%, 95%, and 90%. Based on this stability through time map, potential gene flow among populations was estimated using Circuitscape v5 (McRae et al., 2008).

3 | RESULTS

3.1 | Phylogenetic analysis

Based on the combined datasets (*cytb* and *16S*; 937 bp), the BI consensus and ML bootstrap trees showed *R. pseudodalmatina* as siter group to a clade containing *R. macrocnemis*, *Rana holtzi*, and *R. tavasensis* (Figure S1). Furthermore, the monophyly of *R. pseudodalmatina* is well supported (BS = 99; SH-aLRT = 100; PP = 1.00), and two regional patterns are recognized within the species distribution range in the east (E) and west (W) (Figure S1, Figure 1).

Based on the *cytb* and *16S*, uncorrected genetic distances between E and W groups were low, 0.8% and 0.3%, respectively.

3.2 | Estimating divergence time

Based on the combined mtDNA genes, the MRCA of Hyrcanian/ Anatolia lineage and other species of the genus *Rana* in Europe lived at 13.6 Mya (95% HPD; 6.23–21.11 Mya). At the intra-species level,
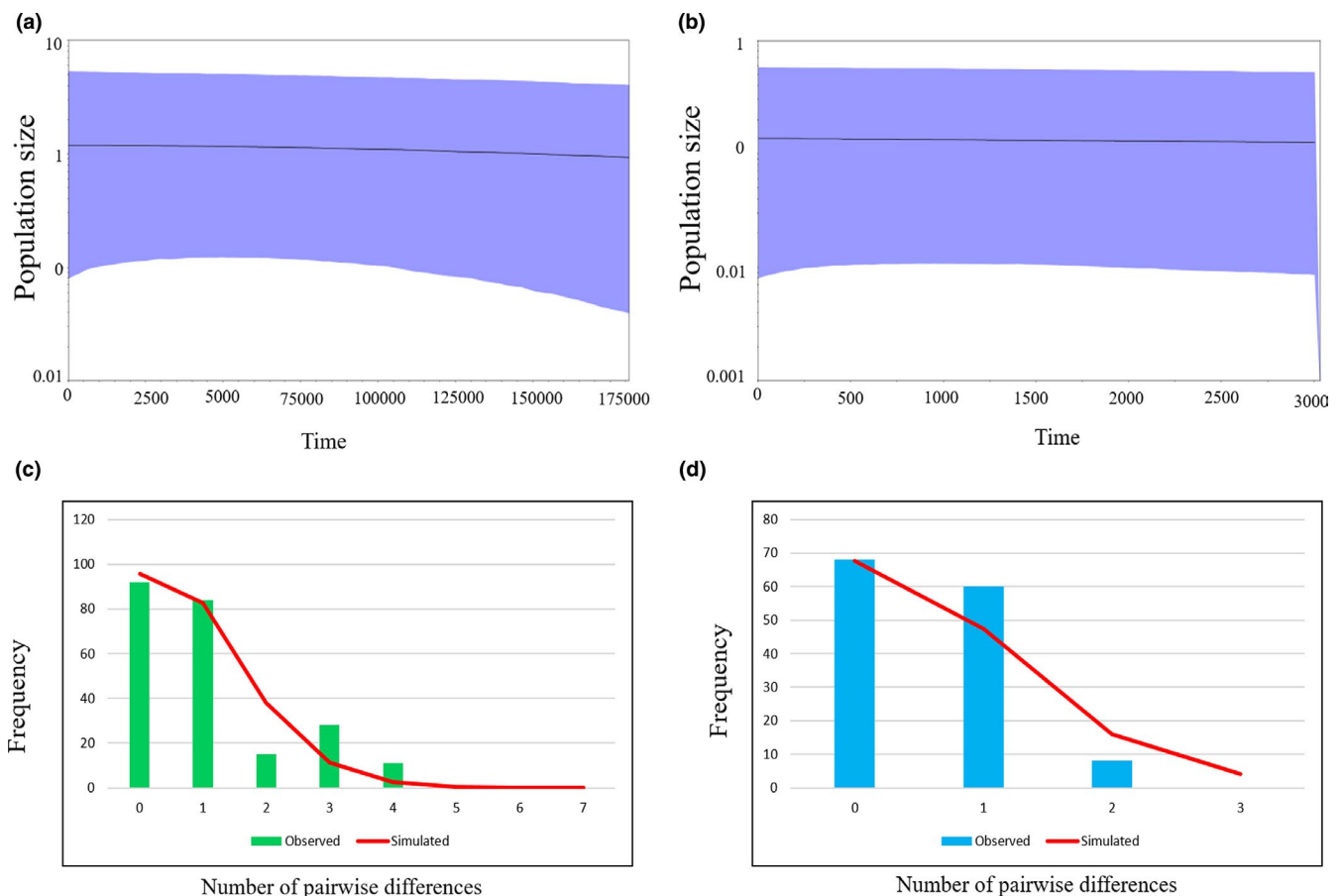
FIGURE 3 Demographic history of two populations of the Hyrcanian wood frog, *Rana pseudodalmatina* based on the *cytb* gene. (a, b) Bayesian Skyline Plots of the western population (a) and the eastern population (b). The central line shows the median values of the population size (1000 years), and the blue area represents the 95% highest posterior density. (c, d) Mismatch distributions of expected frequencies compared to the observed frequencies under the sudden expansion model of population size for the western population (c) and the eastern population (d)

R. pseudodalmatina haplotypes shared a MRCA at 1.6 Mya (95% HPD; 0.58–2.54 Mya; Figure 2).

3.3 | Genetic structure and demographic analysis

Molecular diversity indices based on the *cytb* and *16S* genes including the number of H, *h*, and π within *R. pseudodalmatina* and its regional patterns are presented in Table 1. The *cytb* fragment contained 16 variable sites (12 transitions and four transversions), of which seven were parsimony-informative and nine were singletons. The mean nucleotide composition was A: 22.91%, T: 27.61%, C: 33.76%, and G: 15.73%. The *16S* fragment contained 16 variable sites (14 transitions and two transversions), of which one was parsimony-informative and 15 were singletons. Mean nucleotide composition was A: 29.79%, T: 25.27%, C: 24.33%, and G: 20.61%.

AMOVA results showed significant genetic differences between two regional patterns (E and W) based on mtDNA genes (*cytb*: F_{st} = 0.44, $p < 0.05$; *16S*: F_{st} = 0.58, $p < 0.05$). Most values of Tajima's D and Fu's *Fs* in *R. pseudodalmatina* and its regional patterns were significant and negative (Table 1). The MMD diagrams for the E and W displayed a unimodal pattern with right-skewed consistent with recent demographic expansion (Figure 3c, d). The BSP based on *cytb* showed no obvious trends in N_e through time in each regional pattern (Figure 3a, b). The haplotype parsimony network for the *cytb* gene showed that the western and eastern groups were separated from each other with two-step mutations (Figure 4).

3.4 | Biogeographic analysis

Ancestral distributions of *R. pseudodalmatina* were inferred from S-DIVA and BBM analyses (Figure 5). In both reconstructions, the most recent common ancestor of the species was distributed in the Hyrcanian forests; subsequently, it expanded into the western and eastern areas. According to S-DIVA, a vicariance event took place in the ancestral node of the two areas, and dispersal occurred in the western distribution. BBM reconstruction indicated that vicariance and dispersal events shaped the species' current distribution (Figure 5).

3.5 | Species distribution modeling (past–present–future)

The potential distributions as suggested by our models for past (Last Glacial Maximum, LGM [21 Kya] and Mid-Holocene [6 Kya]), current (1970–2000), and future (2070) climatic conditions are shown in Figure 6, and Figure S2, wherein the average performance was AUC_{test} = 0.828. On average, Temperature Annual Range (BIO7: 57.3%) had the highest contribution, followed by Precipitation of Wettest Month (BIO13: 25.2%), Mean Temperature of Wettest

Quarter (BIO8: 9.0%), and Mean Temperature of Driest Quarter (BIO9: 8.5%).

Based on the SDMs, the central part of the Caspian coast in the southern region was identified as most suitable habitats for *R. pseudodalmatina* during the LGM (Figure 6c). But in the Mid-Holocene, the potential distribution range of the species expanded to include the eastern, central, and western Hyrcanian forests (Figure 6c). Under current climatic conditions, the potential range of the species increased, with habitat suitability uniformly expanding in the Hyrcanian forests from the Talesh region to the Golestan National Park on the southern edge of the Caspian Sea and in the northern slopes of the Alborz Mountains (Figure 6a).

According to the RCPs 2.6, 4.5, 6, and 8.5 scenarios of future climate projections, the distribution range of *R. pseudodalmatina* would tend to shift to higher altitudes especially in the western part of the range in the northern slope of Alborz Mountain (Figure 6e-h).
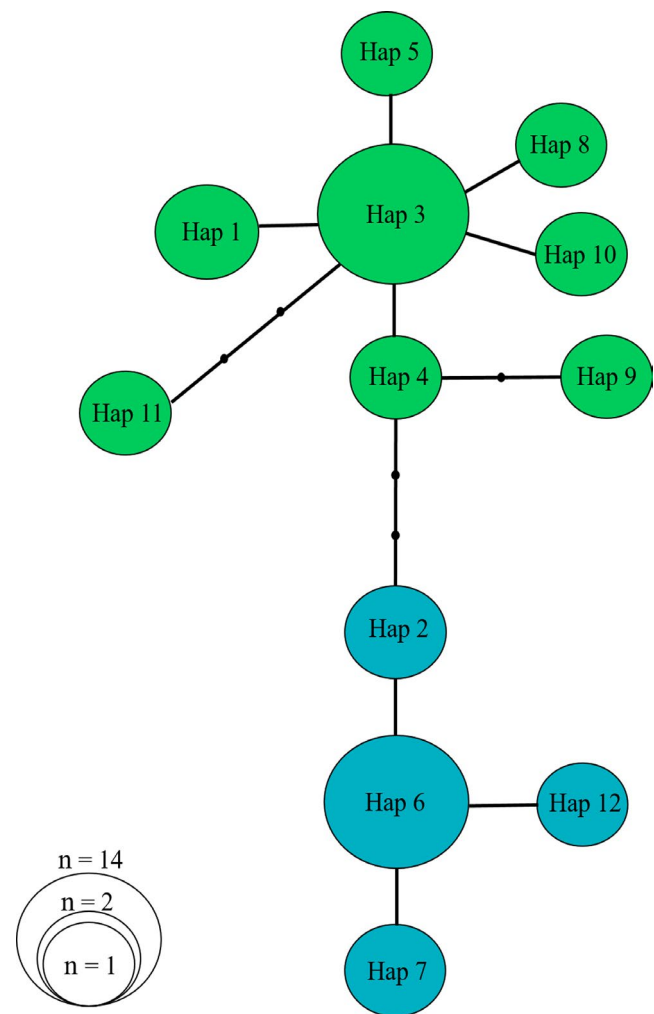
FIGURE 4 Parsimony haplotype network of Hyrcanian wood frog, *Rana pseudodalmatina* based on *cytb* gene. The green and blue colors show individuals of western and eastern populations (see Figure 1). Numbers in circles refer to the haplotype numbers in Appendix 1
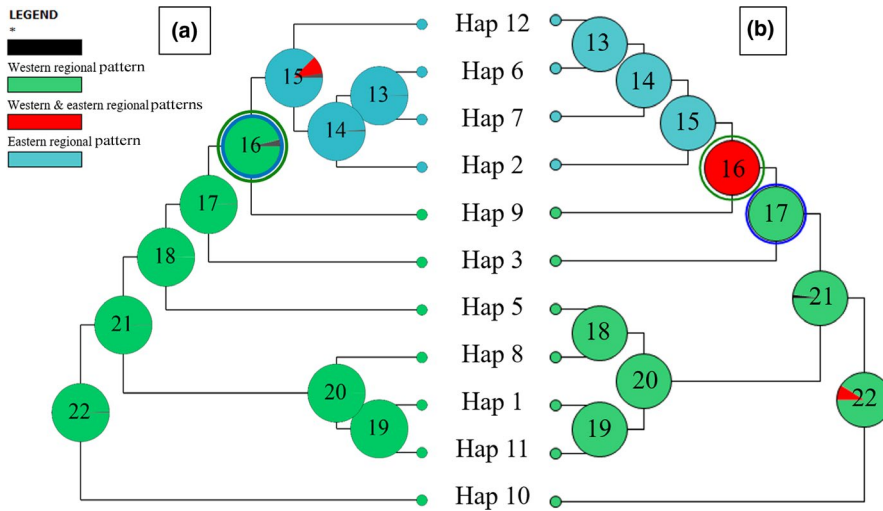
FIGURE 5 The biogeographic analysis of Hyrcanian wood frog, *Rana pseudodalmatina* with BBM (a) and S-DIVA (b) analysis based on *cytb*. For these analyses, two areas were considered (E: blue nodes) the eastern distribution and (W: green nodes) the western distribution. The dark blue and dark green circles around nodes show dispersal and vicariance events, respectively

Stability through time suggests that the Hyrcanian forests acted as historical refugia for this species (Figure 6d). Based on landscape analyses, connectivity under current climatic conditions is maximum in the central part of the range and decreases in the easternmost and westernmost extremes (Figure 7).

4 | DISCUSSION

We examined the genetic diversity patterns of the Hyrcanian wood frog, *R. pseudodalmatina*, throughout its geographic range in the Hyrcanian forests. Also, we used phylogeography and species distribution modeling approaches to investigate the putative glacial refugia and the effect of climate oscillations on the species.

We analyzed two mtDNA genes (*cytb* and *16S*) and found the Hyrcanian/Anatolian lineage and other species of the genus *Rana* in Europe had MRCA during the Miocene (13.6 Mya: 95% HPD; 6.23–21.11 Mya; Figure 2). It is assumed that the uplift of the Turkish–Iranian plateau and the physical vicariance such as the salt-water barrier may have led to the speciation among the Anatolian, the Caucasian, and the Iranian brown frogs (Najibzadeh et al., 2017). *Rana pseudodalmatina* displayed a phylogeographic pattern with two regional groups across its distribution range in the western and eastern Hyrcanian forests (Figure 1, Figure S1). The results of Najibzadeh et al. (2018) corroborate our findings that the species forms two distinct groups in the east and west of the geographic range. However, Najibzadeh et al. (2017) estimate of TMRCA of the two groups is older compared to our findings. Nevertheless, the authors noted that their methodology is prone to misleading results. According to our result, the MRCA of two regional patterns lived 1.6 Mya (95% HPD; 0.58–2.54 Mya), which is much more recent compared to the equivalent estimate of Najibzadeh et al. (2020), which was ca. 4 Mya. This difference is possibly due to the different set of markers, the number of individual samples, prior settings, and calibration points used in the two studies. We used two mtDNA markers (*cytb* and *16S*) for divergence time estimations; however, Najibzadeh et al. (2020) only used the *16S* gene. Our estimated divergence time is comparable to

the Caspian green lizard (*L. strigata*) and Fat Dormouse (*Gilis gilis*) that turned into the eastern and western lineages about 0.9 Mya (95% HPD: 0.55–1.16 Mya) and 1.19 Mya (95% HDP: 0.55–1.91 Mya), respectively, in the Hyrcanian region (Ahmadi et al., 2018; Saberi-Pirooz et al., 2021).

According to the AMOVA results, the two populations are almost isolated from each other because of the F_{st} value of nearly 0.5. The MRCA of the two regional groups of *R. pseudodalmatina* was during the Pleistocene (1.6 Mya [95% HPD; 0.58–2.54 Mya]; Figure 2), which suggests that this species may have been affected by the Quaternary climate fluctuations. It seems that the presence of two groups of *R. pseudodalmatina* in the west and east of the distribution may indicate the long-term residence within two different glacial refugia during the Pleistocene. The existence of cryptic refugia and the idea of "refugia-within-refugia" in the Hyrcanian forests that is proposed here for *R. pseudodalmatina* has been previously discussed for other species that live in this region (Ahmadi et al., 2018; Ahmadzadeh, Flecks, et al., 2013; Saberi-Pirooz et al., 2021). The assessments of demographic history revealed that the recent expansion occurred in the populations (Table 1 and Figure 3).

Our findings identified a successive vicariance event correspond to the divergence of the regional eastern and western groups from the ancestral node (Figure 5). We suggested that the increase in the Caspian Sea water level during the Pleistocene led to the occurrence of vicariance event for the species (Lateef, 1998; Mamedov, 1997). On the other hand, the results of S-DIVA and the BBM analysis showed that dispersal events also played an important role in creating this disjunct distribution pattern (Figure 5). The parsimony haplotype network based on the *cytb* gene indicated that the more derived haplotypes were found in the western region (Figure 4). This suggested that the species derived from the west of the Hyrcanian forests and then migrated to the east of the distribution area.

In response to climate change, species shifted their distribution range to reach more favorable conditions (Guedes et al., 2020). Based on SDMs results, *R. pseudodalmatina* showed a scenario of past range contraction followed by recent expansion (Figure 6 and

FIGURE 6 Potential distribution range of the Hyrcanian wood frog, *Rana pseudodalmatina*, in the Hyrcanian forests under (a) recent, (b) Mid-Holocene (6k), and (c) Last Glacial Maximum, LGM (21k), (d) Stability through time, and future climate projection (2070), (e) RCP 2.6. (f) RCP 4.5. (g) RCP 6. (h) RCP 8.5
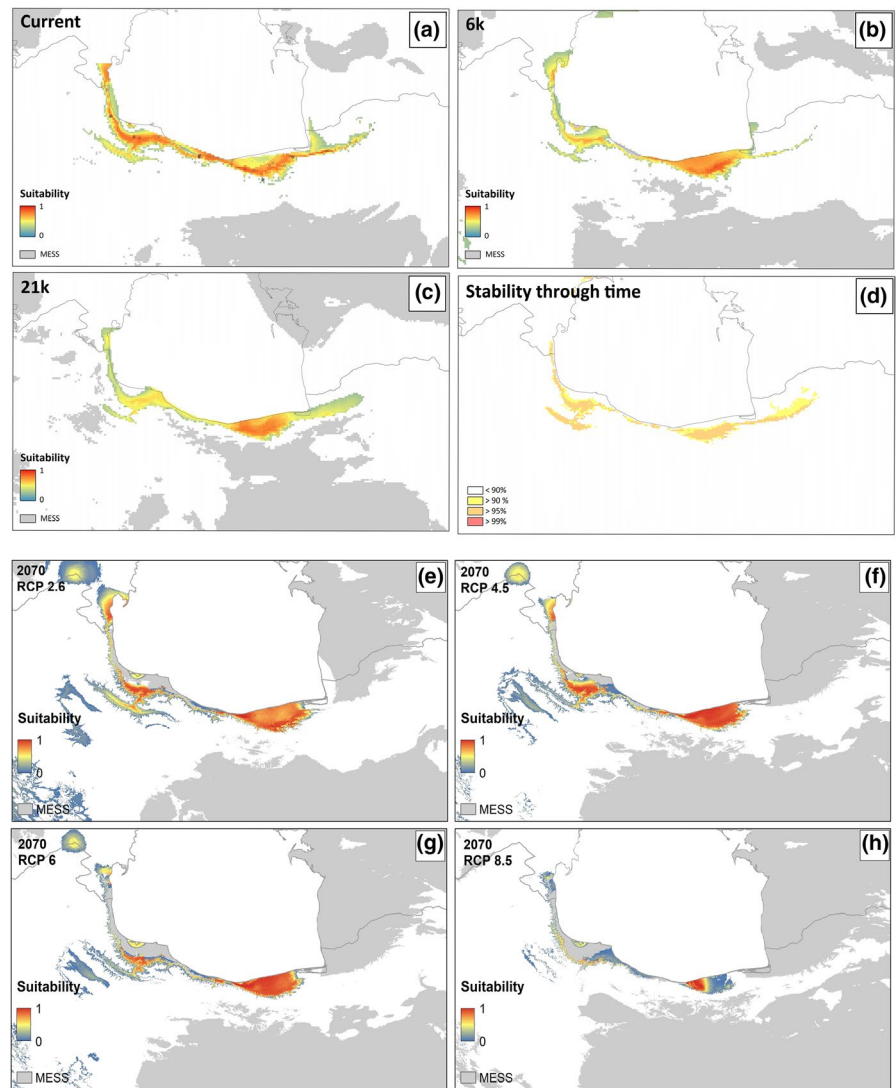
FIGURE 7 Connectivity analysis performed with Circuitscape of the Hyrcanian wood frog, *Rana pseudodalmatina*, in the Hyrcanian forests. The light blue shows the highest connectivity
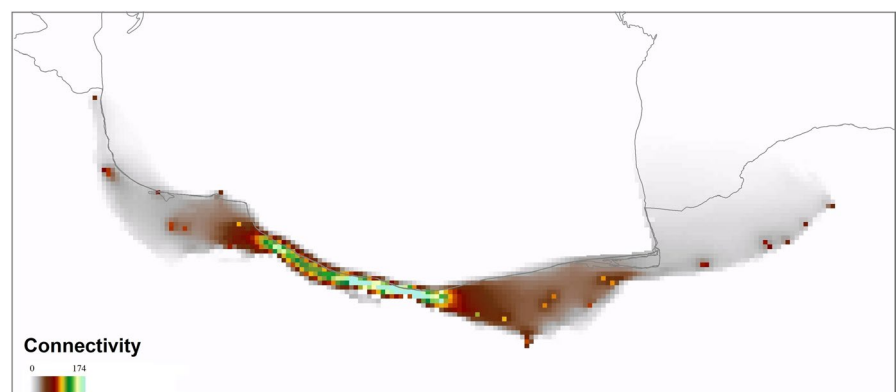

Figure S2). We assumed during the LGM, the distribution of the *R. pseudodalmatina* has been concentrated in two different glacial refugia in the east and west of the distribution range (Figure 6c). Given the warmer conditions since the Mid-Holocene compared to the recent climatic conditions (Akhani et al., 2010), its distribution in the more suitable habitat and a longitudinal shift was expanded throughout the Hyrcanian forests (Figure 6a,b). The longitudinal

shift of the distribution range is also shown in the study of Duan et al. (2016) on Chinese amphibians.

The optimal temperatures for *R. pseudodalmatina* range between 11 and 18°C, and species activity decreases widely at temperatures above 23°C (Pesarakloo et al., 2012). According to our result, Temperature Annual Range (BIO7) had the highest contribution in the model in the past, recent, and future climate change (57.3%).

Based on the future climate (2070) projection, the distribution range of the *R. pseudodalmatina* will shift upward to higher altitudes in the northern slope of Alborz Mountains where the species currently occurs (Figure 6). The results of our study confirm the general trend that amphibian species migrate to higher altitudes under the influence of climate warming. For example, Forero-Medinaet al. (2011) investigated 46 amphibian species of tropical mountains and showed that under future climate changes, their range of distribution will shift to higher altitudes. In contrast to these trends and our findings, Najibzadeh et al. (2020) showed that the suitable habitat for *R. pseudodalmatina* has remained stable since the LGM and will remain the same in the future.

Based on the results of the Circuitscape analysis, the highest connectivity was observed between the populations located in the central parts (the westernmost part of the eastern regional population) to the westward (the easternmost part of the western regional population) of Mazandaran (Figure 7). These results may indicate secondary (postglacial) contact of these populations (Austin et al., 2004; Zamudio & Savage, 2003), which requires further investigation in future studies. According to the results of the stability map through time in this study, Hyrcanian forests acted as climate refugia for the *R. pseudodalmatina* during climate change (Figure 6d). Therefore, Hyrcanian forests may be buffered to contemporary climate change over time and provide resistance to valued socio-cultural, ecological, and physical resources.

CONFLICT OF INTEREST

There are no conflicts of interest.

ORCID

Somaye Vaissi https://orcid.org/0000-0003-3389-1877
Reihaneh Saberi-Pirooz https://orcid.org/0000-0002-9210-3570
Faraham Ahmadzadeh https://orcid.org/0000-0001-7152-8484

REFERENCES

Afroosheh, M., Rödder, D., Mikulicek, P., Akmali, V., Vaissi, S., Fleck, J., Schneide, W., & Sharifi, M. (2019). Mitochondrial DNA variation and quaternary range dynamics in the endangered Yellow Spotted Mountain Newt, *Neurergus derjugini* (Caudata, Salamandridae). *Journal of Zoological Systematics and Evolutionary Research*, *57*(3), 580–590.

Ahmadi, M., Naderi, M., Kaboli, M., Nazarizadeh, M., Karami, M., & Beitollahi, S. M. (2018). Evolutionary applications of phylogenetically-informed ecological niche modelling (ENM) to explore cryptic diversification over cryptic refugia. *Molecular Phylogenetics and Evolution*, *127*, 712–722. https://doi.org/10.1016/j.ympev.2018.06.019

Ahmadzadeh, F., Carretero, M. A., Rödder, D., Harris, D. J., Freitas, S. N., Perera, A., & Böhme, W. (2013). Inferring the effects of past climate fluctuations on the distribution pattern of *Iranolacerta* (Reptilia, Lacertidae): Evidence from mitochondrial DNA and species distribution models. *Zoologischer Anzeiger-A Journal of Comparative Zoology*, *252*(2), 141–148. https://doi.org/10.1016/j.jcz.2012.05.002

Ahmadzadeh, F., Flecks, M., Carretero, M. A., Mozaffari, O., Böhme, W., Harris, D. J., Freitas, S., & Rödder, D. (2013). Cryptic speciation patterns in iranian rock lizards uncovered by integrative taxonomy. *PLoS One*, *8*(12), e80563. https://doi.org/10.1371/journal.pone.0080563

Ahmadzadeh, F., Shahrokhi, G., Saberi-Pirooz, R., Oladi, M., Taati, M., Poyarkov, N., & Rödder, D. (2020). Alborz Heritage: Geographic distribution and genetic differentiation of the Iranian *Paradactylodon* (Amphibia: Hynobiidae). *Amphibia-Reptilia*, *41*(4), 519–534. https://doi.org/10.1163/15685381-bja10022

Akaike, H. (1974). A new look at the statistical model identification. *IEEE Transactions on Automatic Control*, *19*(6), 716–723. https://doi.org/10.1109/TAC.1974.1100705

Akhani, H., Djamali, M., Ghorbanalizadeh, A., & Ramezani, E. (2010). Plant biodiversity of Hyrcanian relict forests, N Iran: An overview of the flora, vegetation, palaeoecology and conservation. *Pakistan Journal of Botany*, *42*, 231–258.

Alroy, J. (2015). Current extinction rates of reptiles and amphibians. *Proceedings of the National Academy of Sciences of the United States of America*, *112*, 201508681. https://doi.org/10.1073/pnas.1508681112.

Anisimova, M., Gil, M., Dufayard, J. F., Dessimoz, C., & Gascuel, O. (2011). Survey of branch support methods demonstrates accuracy, power, and robustness of fast likelihood-based approximation schemes. *Systematic Biology*, *60*, 685–699. https://doi.org/10.1093/sysbio/syr041

Ashrafzadeh, M. R., Kaboli, M., & Naghavi, M. R. (2016). Mitochondrial DNA analysis of Iranian brown bears (*Ursus arctos*) reveals new phylogeographic lineage. *Mammalian Biology*, *81*(1), 1–9. https://doi.org/10.1016/j.mambio.2015.09.001

Austin, J. D., Lougheed, S. C., & Boag, P. T. (2004). Discordant temporal and geographic patterns in maternal lineages of eastern north American frogs, *Rana catesbeiana* (Ranidae) and *Pseudacris crucifer* (Hylidae). *Molecular Phylogenetics and Evolution*, *32*(3), 799–816. https://doi.org/10.1016/j.ympev.2004.03.006

Babik, W., Branicki, W., Sandera, M., Litvinchuk, S., Borkin, L., Irwin, J., & Rafiński, J. (2004). Mitochondrial phylogeography of the moor frog, *Rana arvalis*. *Molecular Ecology*, *13*(6), 1469–1480. https://doi.org/10.1111/j.1365-294X.2004.02157.x

Baek, S. Y., Kang, J. H., Jo, S. H., Jang, J. E., Byeon, S. Y., Wang, J.-H., Lee, H.-G., Choi, J.-K., & Lee, H. J. (2018). Contrasting life histories contribute to divergent patterns of genetic diversity and population connectivity in freshwater sculpin fishes. *BMC Evolutionary Biology*, *18*(1), 52. https://doi.org/10.1186/s12862-018-1171-8

Bao, L., Kudureti, A., Bai, W., Chen, R., Wang, T., Wang, H., & Ge, J. (2015). Contributions of multiple refugia during the last glacial period to current mainland populations of Korean pine (*Pinus koraiensis*). *Scientific Reports*, *5*, 18608. https://doi.org/10.1038/srep18608

Bell, R. C., Parra, J. L., Tonione, M., Hoskin, C. J., Mackenzie, J. B., Williams, S. E., & Moritz, C. (2010). Patterns of persistence and isolation indicate resilience to climate change in montane rainforest lizards. *Molecular Ecology*, *19*(12), 2531–2544. https://doi.org/10.1111/j.1365-294X.2010.04676.x

Bontrager, M., & Angert, A. L. (2019). Gene flow improves fitness at a range edge under climate change. *Evolution Letters*, *3*(1), 55–68. https://doi.org/10.1002/evl3.91

Braconnot, P., Harrison, S. P., Kageyama, M., Bartlein, P. J., Masson-Delmotte, V., Abe-Ouchi, A., Otto-Bliesner, B., & Zhao, Y. (2012). Evaluation of climate models using palaeoclimatic data. *Nature*

Climate Change, *2*(6), 417–424. https://doi.org/10.1038/nclimate1456

Busack, S. D., & Lawson, R. (2008). Morphological, mitochondrial DNA and allozyme evolution in representative amphibians and reptiles inhabiting each side of the Strait of Gibraltar. *Biological Journal of the Linnean Society*, *94*(3), 445–461. https://doi.org/10.1111/j.1095-8312.2008.00992.x

Canestrelli, D., Cimmaruta, R., & Nascetti, G. (2008). Population genetic structure and diversity of the Apennine endemic stream frog, Rana italica–insights on the Pleistocene evolutionary history of the Italian peninsular biota. *Molecular Ecology*, *17*(17), 3856–3872.

Carey, C., & Alexander, M. (2003). Climate change and amphibian declines: Is there a link? *Diversity and Distributions*, *9*, 111–121. https://doi.org/10.1046/j.1472-4642.2003.00011.x

Carnaval, A. C., Hickerson, M. J., Haddad, C. F., Rodrigues, M. T., & Moritz, C. (2009). Stability predicts genetic diversity in the Brazilian Atlantic forest hotspot. *Science*, *323*(5915), 785–789.

Chen, J. H., Huang, C. L., Lai, Y. L., Chang, C. T., Liao, P. C., Hwang, S. Y., & Sun, C. W. (2017). Postglacial range expansion and the role of ecological factors in driving adaptive evolution of *Musa basjoo* var. *formosana*. *Scientific Reports*, *7*(1), 5341. https://doi.org/10.1038/s41598-017-05256-6

Chiocchio, A., Bisconti, R., Zampiglia, M., Nascetti, G., & Canestrelli, D. (2017). Quaternary history, population genetic structure and diversity of the cold-adapted Alpine newt *Ichthyosaura alpestris* in peninsular Italy. *Scientific Reports*, *7*(1), 1–12. https://doi.org/10.1038/s41598-017-03116-x

Clement, M., Posada, D., & Crandall, K. A. (2000). TCS: A computer program to estimate gene genealogies. *Molecular Ecology*, *9*(10), 1657–1659. https://doi.org/10.1046/j.1365-294x.2000.01020.x

Corn, P. (2005). Climate change and amphibians. *Animal Biodiversity and Conservation*, *28*, 59–67.

Cox, K., McKeown, N., Antonini, G., Harvey, D., Solano, E., Van Breusegem, A., & Thomaes, A. (2019). Phylogeographic structure and ecological niche modelling reveal signals of isolation and postglacial colonisation in the European stag beetle. *PLoS One*, *14*(4), e0215860. https://doi.org/10.1371/journal.pone.0215860

Devictor, V., van Swaay, C., Brereton, T., Brotons, L., Chamberlain, D., Heliölä, J., Herrando, S., Julliard, R., Kuussaari, M., Lindström, Å., Reif, J., Roy, D. B., Schweiger, O., Settele, J., Stefanescu, C., Van Strien, A., Van Turnhout, C., Vermouzek, Z., WallisDeVries, M., … Jiguet, F. (2012). Differences in the climatic debts of birds and butterflies at a continental scale. *Nature Climate Change*, *2*(2), 121–124. https://doi.org/10.1038/nclimate1347

Drummond, A. J., & Rambaut, A. (2007). BEAST: Bayesian evolutionary analysis by sampling trees. *BMC Evolutionary Biology*, *7*(1), 1–8. https://doi.org/10.1186/1471-2148-7-214

Drummond, A., Rambaut, A., Shapiro, B., & Pybus, O. G. (2005). Bayesian coalescent inference of past population dynamics from molecular sequences. *Molecular Biology and Evolution*, *22*, 1185–1192. https://doi.org/10.1093/molbev/msi103

Duan, R.-Y., Kong, X.-Q., Huang, M.-Y., Varela, S., & Ji, X. (2016). The potential effects of climate change on amphibian distribution, range fragmentation and turnover in China. *PeerJ*, *4*, e2185. https://doi.org/10.7717/peerj.2185

Duarte, H., Tejedo, M., Katzenberger, M., Marangoni, F., Baldo, D., Beltrán, J. F., Martí, D. A., Richter-Boix, A., & Gonzalez-Voyer, A. (2012). Can amphibians take the heat? Vulnerability to climate warming in subtropical and temperate larval amphibian communities. *Global Change Biology*, *18*(2), 412–421. https://doi.org/10.1111/j.1365-2486.2011.02518.x

Ehl, S., Vences, M., & Veith, M. (2019). Reconstructing evolution at the community level: A case study on Mediterranean amphibians. *Molecular Phylogenetics and Evolution*, *134*, 211–225. https://doi.org/10.1016/j.ympev.2019.02.013

Elith, J., Kearney, M., & Phillips, S. (2010). The art of modelling range-shifting species. *Methods in Ecology and Evolution*, *1*(4), 330–342. https://doi.org/10.1111/j.2041-210X.2010.00036.x

Elith, J., Phillips, S. J., Hastie, T., Dudik, M., Chee, Y. E., & Yates, C. J. (2011). A statistical explanation of MaxEnt for ecologists. *Diversity and Distributions*, *17*(1), 43–57. https://doi.org/10.1111/j.1472-4642.2010.00725.x

Excoffier, L., & Lischer, H. (2010). ARLEQUIN suite ver 3.5: A new series of programs to perform population genetics analyses under Linux and Windows. *Molecular Ecology Resources*, *10*, 564–567. https://doi.org/10.1111/j.1755-0998.2010.02847.x

Fick, S. E., & Hijmans, R. J. (2017). WorldClim 2: New 1-km spatial resolution climate surfaces for global land areas. *International Journal of Climatology*, *37*(12), 4302–4315. https://doi.org/10.1002/joc.5086

Foden, W. B., Butchart, S. H. M., Stuart, S. N., Vié, J.-C., Akçakaya, H. R., Angulo, A., DeVantier, L. M., Gutsche, A., Turak, E., Cao, L., Donner, S. D., Katariya, V., Bernard, R., Holland, R. A., Hughes, A. F., O'Hanlon, S. E., Garnett, S. T., Şekercioğlu, Ç. H., & Mace, G. M. (2013). Identifying the world's most climate change vulnerable species: A systematic trait-based assessment of all birds, amphibians and corals. *PLoS One*, *8*(6), e65427. https://doi.org/10.1371/journal.pone.0065427

Forero-Medina, G., Joppa, L., & Pimm, S. L. (2011). Constraints to species' elevational range shifts as climate changes. *Conservation Biology*, *25*(1), 163–171. https://doi.org/10.1111/j.1523-1739.2010.01572.x

Fouquet, A., Noonan, B., Rodrigues, M., Pech, N., Gilles, A., & Gemmell, N. (2012). Multiple Quaternary refugia in the eastern Guiana Shield revealed by comparative phylogeography of 12 frog species. *Systematic Biology*, *61*, 461–489. https://doi.org/10.1093/sysbio/syr130

Gamisch, A. (2019). Oscillayers: A dataset for the study of climatic oscillations over Plio-Pleistocene time-scales at high spatial-temporal resolution. *Global Ecology and Biogeography*, *28*(11), 1552–1560. https://doi.org/10.1111/geb.12979

Guedes, D., Arenas-Castro, S., & Sillero, N. (2020). Ecological niche models reveal climate change effect on biogeographical regions: The Iberian Peninsula as a case study. *Climate*, *8*, 42.

He, J., Yan, C., Holyoak, M., Wan, X., Ren, G., Hou, Y., Xie, Y., & Zhang, Z. (2018). Quantifying the effects of climate and anthropogenic change on regional species loss in China. *PLoS One*, *13*(7), e0199735. https://doi.org/10.1371/journal.pone.0199735

Hillis, D. M., & Wilcox, T. P. (2005). Phylogeny of the New World true frogs (*Rana*). *Molecular Phylogenetics and Evolution*, *34*(2), 299–314. https://doi.org/10.1016/j.ympev.2004.10.007

Hopley, T., & Byrne, M. (2019). Gene flow and genetic variation explain signatures of selection across a climate gradient in two Riparian species. *Genes*, *10*(8), 579. https://doi.org/10.3390/genes10080579

Hua, X., & Wiens, J. J. (2013). How does climate influence speciation? *The American Naturalist*, *182*, 1–12. https://doi.org/10.1086/670690

Huelsenbeck, J. P., & Ronquist, F. (2001). MRBAYES: Bayesian inference of phylogenetic trees. *Bioinformatics*, *17*(8), 754–755. https://doi.org/10.1093/bioinformatics/17.8.754

Igea, J., Aymerich, P., Fernández-González, A., González-Esteban, J., Gómez, A., Alonso, R., Gosálbez, J., & Castresana, J. (2013). Phylogeography and postglacial expansion of the endangered semi-aquatic mammal *Galemys pyrenaicus*. *BMC Evolutionary Biology*, *13*(1), 115. https://doi.org/10.1186/1471-2148-13-115

Katoh, K., Rozewicki, J., & Yamada, K. D. (2017). MAFFT online service: Multiple sequence alignment, interactive sequence choice and visualization. *Briefings in Bioinformatics*, *20*(4), 1160–1166. https://doi.org/10.1093/bib/bbx108

Kocher, T. D., Thomas, W. K., Meyer, A., Edwards, S. V., Pääbo, S., Villablanca, F. X., & Wilson, A. C. (1989). Dynamics of mitochondrial DNA evolution in animals: Amplification and sequencing with conserved primers. *Proceedings of the National Academy of Sciences*

of the United States of America, 86(16), 6196–6200. https://doi.org/10.1073/pnas.86.16.6196

Krehenwinkel, H., Graze, M., Rodder, D., Tanaka, K., Baba, Y. G., Muster, C., & Uhl, G. (2016). A phylogeographical survey of a highly dispersive spider reveals eastern Asia as a major glacial refugium for Palaearctic fauna. *Journal of Biogeography*, 43(8), 1583–1594. https://doi.org/10.1111/jbi.12742

Lateef, A. (1998). *Some notes on the middle-late quaternary history of the Caspian sea-level changes*. Beirut, Lebanon: Paper presented at the 4th International Conference on the Geology of the Middle East.

Leipold, M., Tausch, S., Poschlod, P., & Reisch, C. (2017). Species distribution modeling and molecular markers suggest longitudinal range shifts and cryptic northern refugia of the typical calcareous grassland species Hippocrepis comosa (*horseshoe vetch*). *Ecology and Evolution*, 7(6), 1919–1935.

Liepelt, S., Cheddadi, R., de Beaulieu, J.-L., Fady, B., Gömöry, D., Hussendörfer, E., Konnert, M., Litt, T., Longauer, R., Terhürne-Berson, R., & Ziegenhagen, B. (2009). Postglacial range expansion and its genetic imprints in *Abies alba* (Mill.) — A synthesis from palaeobotanic and genetic data. *Review of Palaeobotany and Palynology*, 153(1), 139–149. https://doi.org/10.1016/j.revpalbo.2008.07.007

Lymberakis, P., Poulakakis, N., Manthalou, G., Tsigenopoulos, C. S., Magoulas, A., & Mylonas, M. (2007). Mitochondrial phylogeography of Rana (*Pelophylax*) populations in the Eastern Mediterranean region. *Molecular Phylogenetics and Evolution*, 44(1), 115–125. https://doi.org/10.1016/j.ympev.2007.03.009

Malekoutian, M., Sharifi, M., & Vaissi, S. (2020). Mitochondrial DNA sequence analysis reveals multiple Pleistocene glacial refugia for the Yellow-spotted mountain newt, *Neurergus derjugini* (Caudata: Salamandridae) in the mid-Zagros range in Iran and Iraq. *Ecology and Evolution*, 10(5), 2661–2676.

Mamedov, A. (1997). The late Pleistocene-Holocene history of the Caspian Sea. *Quaternary International*, 41, 161–166. https://doi.org/10.1016/S1040-6182(96)00048-1

McCarty, J. P. (2001). Ecological consequences of recent climate change. *Conservation Biology*, 15(2), 320–331. https://doi.org/10.1046/j.1523-1739.2001.015002320.x

McRae, B. H., Dickson, B. G., Keitt, T. H., & Shah, V. B. (2008). Using circuit theory to model connectivity in ecology, evolution, and conservation. *Ecology*, 89(10), 2712–2724. https://doi.org/10.1890/07-1861.1

Najibzadeh M., Ehl S., Feldmeier S., Pesarakloo A., Veith M. (2021). Unequal sisters – Past and potential future range development of Anatolian and Hyrcanian brown frogs. *Zoology*, 144, 125873. https://doi.org/10.1016/j.zool.2020.125873

Najibzadeh, M., Gharzi, A., Rastegar-Pouyani, N., Rastegar-Pouyani, E., & Pesarakloo, A. (2018). Genetic structure of the hyrcanian wood frog, *Rana pseudodalmatina* (Amphibia: Ranidae) using mtDNA gene sequences. *Russian Journal of Genetics*, 54(10), 1221–1228. https://doi.org/10.1134/S1022795418100095

Najibzadeh, M., Veith, M., Gharzi, A., Rastegar-Pouyani, N., Rastegar-Pouyani, E., Kieren, S., & Pesarakloo, A. (2017). Molecular phylogenetic relationships among Anatolian-Hyrcanian brown frog taxa (Ranidae: *Rana*). *Amphibia-Reptilia*, 38(3), 339–350. https://doi.org/10.1163/15685381-00003114

Nguyen, L.-T., Schmidt, H. A., von Haeseler, A., & Minh, B. Q. (2015). IQ-TREE: A fast and effective stochastic algorithm for estimating maximum likelihood phylogenies. *Molecular Biology and Evolution*, 32, 268–274. https://doi.org/10.1093/molbev/msu300

Nicolas, V., Mataame, A., Crochet, P. A., Geniez, P., Fahd, S., & Ohler, A. (2018). Phylogeography and ecological niche modeling unravel the evolutionary history of the African green toad, *Bufotes boulengeri boulengeri* (Amphibia: Bufonidae), through the Quaternary. *Journal of Zoological Systematics and Evolutionary Research*, 56(1), 102–116.

Nylander, J. (2004). *MrModeltest version 2. Program distributed by the author*. Uppsala University.

Omann, I., Stocker, A., & Jäger, J. (2009). Climate change as a threat to biodiversity: An application of the DPSIR approach. *Ecological Economics*, 69(1), 24–31. https://doi.org/10.1016/j.ecolecon.2009.01.003

Ortiz-Yusty, C., Páez, V., & Zapata, F. (2013). Temperature and precipitation as predictors of species richness in Northern Andean amphibians from Colombia. *Caldasia*, 35, 65–80.

Palumbi, S., Martin, A., Romano, S., McMillan, W., Stice, L., & Grabowski, G. (1991). *The simple fool's guide to PCR. Version 2*. University of Hawaii. Zoology Department.

Pesarakloo, A., Gharzi, A., Gholi-Kami, H., & Najibzadeh, M. (2012). An investigation on the reproductive biology of *Rana macrocnemis pseudodalmatina* (Amphibians: Anura) in Golestan province (Minudasht). *Iranian Journal of Biology*, 25(1), 55–63.

Peso-Fernández, M., Ponti de la Iglesia, R., Ponz Segrelles, G., Gonzalez Martinez, R., Arcones Segovia, A., & Vieites, D. R. (2016). The complete mitochondrial genome of the Endangered European brown frog *Rana pyrenaica* through RNAseq. *Mitochondrial DNA Part B*, 1(1), 394–396.

Phillips, S. J., Anderson, R. P., Dudik, M., Schapire, R. E., & Blair, M. E. (2017). Opening the black box: An open-source release of Maxent. *Ecography*, 40(7), 887–893. https://doi.org/10.1111/ecog.03049

Phillips, S. J., Anderson, R. P., & Schapire, R. E. (2006). Maximum entropy modeling of species geographic distributions. *Ecological Modelling*, 190, 231–259. https://doi.org/10.1016/j.ecolmodel.2005.03.026

Pounds, J. A., Bustamante, M. R., Coloma, L. A., Consuegra, J. A., Fogden, M. P., Foster, P. N., … Puschendorf, R. (2006). Widespread amphibian extinctions from epidemic disease driven by global warming. *Nature*, 439(7073), 161–167.

Provan, J., & Bennett, K. (2008). Phylogeographic insights into cryptic glacial refugia. *Trends in Ecology and Evolution*, 23(10), 564–571. https://doi.org/10.1016/j.tree.2008.06.010

Rambaut, A., Drummond, A., & Suchard, M. (2007). *Tracer v1.6*. http://beast.bio.ed.ac.uk. In: Tracer.

Razgour, O., Forester, B., Taggart, J. B., Bekaert, M., Juste, J., Ibáñez, C., Puechmaille, S. J., Novella-Fernandez, R., Alberdi, A., & Manel, S. (2019). Considering adaptive genetic variation in climate change vulnerability assessment reduces species range loss projections. *Proceedings of the National Academy of Sciences of the United States of America*, 116(21), 10418–10423. https://doi.org/10.1073/pnas.1820663116

Rodriguez, F., Oliver, J. L., Marin, A., & Medina, J. R. (1990). The general stochastic model of nucleotide substitution. *Journal of Theoretical Biology*, 142(4), 485–501. https://doi.org/10.1016/S0022-5193(05)80104-3

Röhrig, E. (1991). Deciduous forests of the Near East. *Ecosystems of the World*, 7, 527–537

Saberi-Pirooz, R., Ahmadzadeh, F., Ataei, S., Taati, M., Qashqaei, A. T., & Carretero, M. A. (2018). A phylogenetic assessment of the meadow lizard *Darevskia praticola* (Eversmann, 1834) from Iran. *Zootaxa*, 4441(1), 46–58.

Saberi-Pirooz, R., Rajabi-Maham, H., Ahmadzadeh, F., Kiabi, B. H., Javidkar, M., Carretero, M. A. (2021). Pleistocene climate fluctuations as the major driver of genetic diversity and distribution patterns of the Caspian green lizard, Lacerta strigata Eichwald, 1831. *Ecology and Evolution*, 1–14. https://doi.org/10.1002/ece3.7543

Safner, T., Miaud, C., Gaggiotti, O., Decout, S., Rioux, D., Zundel, S., & Manel, S. (2011). Combining demography and genetic analysis to assess the population structure of an amphibian in a human-dominated landscape. *Conservation Genetics*, 12(1), 161–173. https://doi.org/10.1007/s10592-010-0129-1

Sambrook, H. (1989). *Molecular cloning: A laboratory manual*. Cold Spring Harbor.

Schierenbeck, K. A. (2017). Population-level genetic variation and climate change in a biodiversity hotspot. *Annals of Botany*, 119(2), 215–228. https://doi.org/10.1093/aob/mcw214

Sharifi, M., Shafiei Bafti, S., Papenfuss, T., Anderson, S., & Nilson, G. (2009). *Rana pseudodalmatina. The IUCN red list of threatened species 2009*: e.T61874A12557550. https://dx.doi.org/10.2305/IUCN.UK.2009.RLTS.T61874A12557550.en

Shimodaira, H., & Hasegawa, M. (1999). Multiple comparisons of log-likelihoods with applications to phylogenetic inference. *Molecular Biology and Evolution*, 16, 1114–1116. https://doi.org/10.1093/oxfordjournals.molbev.a026201

Song, W., Cao, L.-J., Li, B.-Y., Gong, Y.-J., Hoffmann, A. A., & Wei, S.-J. (2018). Multiple refugia from penultimate glaciations in East Asia demonstrated by phylogeography and ecological modelling of an insect pest. *BMC Evolutionary Biology*, 18(1), 152. https://doi.org/10.1186/s12862-018-1269-z

Stamatakis, A. (2006). RAxML-VI-HPC: Maximum likelihood-based phylogenetic analyses with thousands of taxa and mixed models. *Bioinformatics*, 22(21), 2688–2690. https://doi.org/10.1093/bioinformatics/btl446

Swets, J. A. (1988). Measuring the accuracy of diagnostic systems. *Science*, 240(4857), 1285–1293.

Swofford, D. (2002). *Phylogenetic analysis using parsimony (* and other methods). Version 4*. Sinauer Associates.

Tohidifar, M., Moser, M., Zehzad, B., & Ghadirian, T. (2016). *Biodiversity of the Hyrcanian Forests: A synthesis report*. (1–41). Iran: UNDP/GEF/FRWO Caspian Hyrcanian Forest Project.

Urban, M. C. (2015). Accelerating extinction risk from climate change. *Science*, 348(6234), 571–573.

Veith, M., Schmidtler, J., Kosuch, J., Baran, I., & Seitz, A. (2003). Palaeoclimatic changes explain Anatolian mountain frog evolution: A test for alternating vicariance and dispersal events. *Molecular Ecology*, 12(1), 185–199. https://doi.org/10.1046/j.1365-294X.2003.01714.x

Velásquez-Tibata, J., Salaman, P., & Graham, C. (2012). Effects of climate change on species distribution, community structure, and conservation of birds in protected areas in Colombia. *Regional Environmental Change*, 13, 235–248. https://doi.org/10.1007/s10113-012-0329-y

Velo-Antón, G., Parra, J., Parra-Olea, G., & Zamudio, K. (2013). Tracking climate change in a dispersal-limited species: Reduced spatial and genetic connectivity in a montane salamander. *Molecular Ecology*, 22(12), 3261–3278. https://doi.org/10.1111/mec.12310

Vences, M. (1999). *Phylogenetic studies on Ranoid Frogs (Amphibia: Anura): With a discussion of the origin and evolution of the vertebrate clades of Madagascar*. Doctoral dissertation, Rheinische Friedrich-Wilhelms-Universität zu Bonn.

Vieira, K. S., Montenegro, P. F. G., Santana, G. G., & da Silva Vieira, W. L. (2018). Effect of climate change on distribution of species of common horned frogs in South America. *PLoS One*, 13(9), e0202813. https://doi.org/10.1371/journal.pone.0202813

Vignali, S., Barras, A., & Braunisch, V. (2020). *SDMtune: Species distribution model selection. R package version 1.1.0*. https://github.com/ConsBiol-unibern/SDMtune

Wake, D. B., & Vredenburg, V. T. (2008). Are we in the midst of the sixth mass extinction? A view from the world of amphibians. *Proceedings of the National Academy of Sciences*, 105(Supplement 1), 11466–11473. https://doi.org/10.1073/pnas.0801921105

Yang, Z. (1996). Among-site rate variation and its impact on phylogenetic analyses. *Trends in Ecology and Evolution*, 11(9), 367–372. https://doi.org/10.1016/0169-5347(96)10041-0

Yodthong, S., Cameron, D., Prasankok, P., & Aowphol, A. (2015). Phylogenetic patterns of the Southeast Asian tree frog *Chiromantis hansenae* in Thailand. *Asian Herpetological Research*, 5(3), 179–196.

Yu, Y., Harris, A., Blair, C., & He, X.-J. (2015). RASP (Reconstruct Ancestral State in Phylogenies): A tool for historical biogeography. *Molecular Phylogenetics and Evolution*, 87, 46–49. https://doi.org/10.1016/j.ympev.2015.03.008

Yuan, Z. Y., Zhou, W. W., Chen, X., Poyarkov, N. A. Jr, Chen, H. M., Jang-Liaw, N. H., ... Che, J. (2016). Spatiotemporal diversification of the true frogs (genus *Rana*): A historical framework for a widely studied group of model organisms. *Systematic Biology*, 65(5), 824–842.

Zamudio, K. R., & Savage, W. K. (2003). Historical isolation, range expansion, and secondary contact of two highly divergent mitochondrial lineages in spotted salamanders (*Ambystoma maculatum*). *Evolution*, 57(7), 1631–1652. https://doi.org/10.1111/j.0014-3820.2003.tb00370.x

Zeisset, I., & Beebee, T. J. C. (2008). Amphibian phylogeography: A model for understanding historical aspects of species distributions. *Heredity*, 101(2), 109–119. https://doi.org/10.1038/hdy.2008.30

Zhang, Y.-H., Zhao, Y.-Y., Li, X.-Y., & Li, X.-C. (2016). Evolutionary history and population genetic structure of the endemic tree frog *Hyla tsinlingensis* (Amphibia: Anura: Hylidae) inferred from mitochondrial gene analysis. *Mitochondrial DNA Part A*, 27(2), 1348–1357.

Zhao, M., Chang, Y., Kimball, R. T., Zhao, J., Lei, F., & Qu, Y. (2019). Pleistocene glaciation explains the disjunct distribution of the Chestnut-vented Nuthatch (Aves, Sittidae). *Zoologica Scripta*, 48(1), 33–45. https://doi.org/10.1111/zsc.12327

Zhou, W.-W., Zhang, B.-L., Chen, H.-M., Jin, J.-Q., Yang, J.-X., Wang, Y.-Y., Jiang, K. E., Murphy, R. W., Zhang, Y.-P., & Che, J. (2014). DNA barcodes and species distribution models evaluate threats of global climate changes to genetic diversity: A case study from Nanorana parkeri (Anura: Dicroglossidae). *PLoS One*, 9, e103899. https://doi.org/10.1371/journal.pone.0103899

SUPPORTING INFORMATION

Additional supporting information may be found online in the Supporting Information section.

Figure S1. A phylogenetic tree of Ranidae based on the concatenated genes (*cytb* and *16S*).

Figure S2. Animation showing the changes in the potential distribution according to projections to oscillayers estimates.

Table S1. Details of the primers used in the study.

Alignment S1. Alignment of *cytb*, consisting of 442 base pairs and 61 sequences that composed the final dataset.

Alignment S2. Alignment of *16S*, consisting of 495 base pairs and 66 sequences that composed the final dataset.

APPENDIX 1

The dataset of *Rana* used in this study. The information includes code ID, haplotype number for *cytb* (HT *cytb*), locality, origin, geographical coordinates and the accession numbers for two mtDNA (*cytb* and *16S*) genes

Taxon					GenBank accession numbers	
code ID	HT *cytb*	Locality/Country	Lat (N)/Long (E)	Origin	16S	cytb
Rana pseudodalmatina						
ES365	—	Iran/Golestan	37.035/55.03	This study	MT864022	—
ES347	Hap 2	Iran/Golestan	36.9944/55.0599	This study	MT864026	MW017119
ES349	—	Iran/Mazandaran	36.533/51.532	This study	MT864010	—
ES363	Hap 3	Iran/Mazandaran	36.225/51.366	This study	MT864012	MW017121
ES320	Hap 4	Iran/Mazandaran	36.662/51.184	This study	MT864028	MW017117
ES341	—	Iran/Mazandaran	36.369/51.133	This study	MT864009	—
ES344	Hap 6	Iran/Mazandaran	36.458/52.997	This study	MT864019	MW017118
ES346	—	Iran/Mazandaran	36.365/52.36	This study	MT864020	—
ES348	Hap 6	Iran/Mazandaran	36.68/53.53	This study	MT864021	MW017120
ES366	Hap 6	Iran/Mazandaran	36.57/52.032	This study	MT864023	MW017122
ES795	Hap 2	Iran/Mazandaran	36.082/52.823	This study	MT864015	MW017125
ES804	—	Iran/Mazandaran	36.523/51.091	This study	MT864016	—
ES806	Hap 7	Iran/Mazandaran	36.089/36.089	This study	MT864024	MW017126
ES814	—	Iran/Mazandaran	36.654/53.598	This study	MT864025	—
ES813	—	Iran/Mazandaran	36.67/51.188	This study	MT864017	—
—	Hap 3	Iran/Mazandaran	—	Veith et al. (2003)	—	AY147969
ES384	Hap 1	Iran/Gilan	36.992/50.081	This study	MT864011	MW017123
ES385	—	Iran/Gilan	36.992/50.081	This study	MT864013	—
ES816	Hap 3	Iran/Gilan	37.137/49.665	This study	MT864018	MW017127
ES429	Hap 5	Iran/Gilan	37.66/48.92	This study	MT864014	MW017124
ES430	—	Iran/Gilan	37.67/48.91	This study	MT864027	—
RUZM.R.R13.1	Hap 6	Iran/Loveh	37.35/55.65	Najibzadeh et al. (2018)	MF344713	MF344774
RUZM.R.R13.2	Hap 6	Iran/Loveh	37.35/55.65	Najibzadeh et al. (2018)	MF344714	MF344775
RUZM.R.R13.3	Hap 6	Iran/Loveh	37.35/55.65	Najibzadeh et al. (2018)	MF344715	MF344776
RUZM.R.R13.4	Hap 6	Iran/Loveh	37.35/55.65	Najibzadeh et al. (2018)	MF344712	MF344773
RUZM.R.R13.5	Hap 6	Iran/Behshahr	36.66/53.59	Najibzadeh et al. (2018)	MF344716	MF344777
RUZM.R.R13.6	Hap 6	Iran/Behshahr	36.66/53.59	Najibzadeh et al. (2018)	MF344717	MF344778
RUZM.R.R13.7	Hap 6	Iran/Behshahr	36.66/53.59	Najibzadeh et al. (2018)	MF344718	MF344779
RUZM.R.R13.8	Hap 6	Iran/Behshahr	36.66/53.59	Najibzadeh et al. (2018)	MF344719	MF344780
RUZM.R.R13.9	Hap 8	Iran/Rasht	37.15/49.52	Najibzadeh et al. (2018)	MF344720	MF344781
RUZM.R.R13.11	Hap 3	Iran/Rasht	37.15/49.52	Najibzadeh et al. (2018)	MF344721	MF344782
RUZM.R.R13.12	Hap 3	Iran/Rasht	37.15/49.52	Najibzadeh et al. (2018)	MF344722	MF344783
RUZM.R.R13.13	Hap 3	Iran/Rasht	37.15/49.52	Najibzadeh et al. (2018)	MF344723	MF344784
RUZM.R.R13.14	Hap 9	Iran/Rasht	37.15/49.52	Najibzadeh et al. (2018)	MF344724	MF344785
RUZM.R.R13.15	Hap 3	Iran/Rasht	37.15/49.52	Najibzadeh et al. (2018)	MF344725	MF344786
RUZM.R.R13.16	Hap 3	Iran/Salmanshahr	36.64/51.19	Najibzadeh et al. (2018)	MF344726	MF344787
RUZM.R.R13.17	Hap 3	Iran/Salmanshahr	36.64/51.19	Najibzadeh et al. (2018)	MF344727	MF344788
RUZM.R.R13.18	Hap 10	Iran/Astara	38.34/48.83	Najibzadeh et al. (2018)	MF344728	MF344789
RUZM.R.R13.19	Hap 3	Iran/Astara	38.34/48.83	Najibzadeh et al. (2018)	MF344729	MF344790
RUZM.R.R13.21	Hap 3	Iran/Astara	38.34/48.83	Najibzadeh et al. (2018)	MF344730	MF344791
RUZM.R.R13.22	Hap 3	Iran/Astara	38.34/48.83	Najibzadeh et al. (2018)	MF344731	MF344792

(Continues)

APPENDIX 1 (Continued)

Taxon					GenBank accession numbers	
code ID	HT *cytb*	Locality/Country	Lat (N)/Long (E)	Origin	*16S*	*cytb*
RUZM.R.R13.23	Hap 11	Iran/Astara	38.34/48.83	Najibzadeh et al. (2018)	MF344732	MF344793
RUZM.R.R13.24	Hap 3	Iran/Astara	38.34/48.83	Najibzadeh et al. (2018)	MF344733	MF344794
RUZM.R.R13.25	Hap 6	Iran/Sari	36.33/52.60	Najibzadeh et al. (2018)	MF344735	MF344796
RUZM.R.R13.26	Hap 7	Iran/Sari	36.33/52.60	Najibzadeh et al. (2018)	MF344736	MF344797
RUZM.R.R13.27	Hap 12	Iran/Sari	36.33/52.60	Najibzadeh et al. (2018)	MF344734	MF344795
RUZM.R.R13.28	Hap 3	Iran/Langarud	37.17/50.16	Najibzadeh et al. (2018)	MF344737	MF344798
RUZM.R.R13.29	Hap 1	Iran/Langarud	37.17/50.16	Najibzadeh et al. (2018)	MF344738	MF344799
Rana macrocnemis						
ES405		Iran/Azerbijan		This study	MZ171537	MW017128
ES407		Iran/Azerbijan		This study	—	MW017129
ES416		Iran/Azerbijan		This study	MZ171538	MW017130
ES419		Iran/Azerbijan		This study	MZ171539	MW017131
ES420		Iran/Azerbijan		This study	MZ171540	MW017132
				Veith et al. (2003)	AY147940	AY147960
Rana arvalis arvalis				Veith et al. (2003)	AY147938	AY147958
Rana arvalis wolterstorffi				Veith et al. (2003)	AY147939	AY147959
Rana macrocnemis				Veith et al. (2003)	AY147940	AF373151
Rana dalmatina				Veith et al. (2003)	AY147944	AY147962
Rana graeca				Veith et al. (2003)	AY147945	—
Rana holtzi				Veith et al. (2003)	AY147946	AY147964
Rana iberica				Veith et al. (2003)	AY147947	AY147965
Rana pyrenaica				Peso-Fernández et al. (2016)	KU720300	KU720300
Rana temporaria temporaria				Veith et al. (2003)	AY147956	AY147977
Rana temporaria parvipalmata				Veith et al. (2003)	AY147955	AY147976
Rana temporaria canigonensis				Veith et al. (2003)	AY147952	AY147973
Rana temporaria honnorati				Veith et al. (2003)	AY147954	AY147975
Rana italica				Veith et al. (2003)	AY147948	—
Rana italica				Canestrelli et al. (2008)	—	EU595505
Rana latastei				Veith et al. (2003)	AY147949	AY147967
Rana asiatica				Yuan et al. (2016)	KX269200	KX269346
Rana dalmatina				Canestrelli et al. (2014)	—	KJ789718
Rana italica				Canestrelli et al. (2008)	—	EU595490
Rana tavasensis				Veith et al. (2003)	—	AY147970
Rana berlandieri				Hillis and Wilcox (2005)/ Yuan et al. (2016)	AY779235	KX269301
Rana dunni				Hillis and Wilcox (2005)/ Yuan et al. (2016)	AY779222	KX269305
Rana clamitans				Hillis and Wilcox (2005)/ Yuan et al. (2016)	AY779204	KX269304
Rana septentrionalis				Yuan et al. (2016)	KX269179	KX269314

(Continues)

APPENDIX 1 (Continued)

Taxon					GenBank accession numbers	
code ID	HT *cytb*	Locality/Country	Lat (N)/Long (E)	Origin	*16S*	*cytb*
Pelophylax bedriagae				Hofman et al. (2016)	NC-029200	NC-029200
Pelophylax perezi				Vences (1999)/Busack and Lawson (2008)	AF215424	DQ902145
Pelophylax saharica				Lymberakis et al. (2007)	DQ474229	DQ902147
Pelophylax cretensis				Hofman et al. (2016)	NC-025575	NC-025575